1

Analysis of Thermodynamic and Phononic Properties of Perovskite Manganites

Renu Choithrani
Department of Physics, Barkatullah University, Bhopal
India

1. Introduction

The perovskite manganites are of recognized importance, owing to the development of new materials designed for different potential scientific and technological applications, such as *magnetic sensors in the tracking and location of emergency personnel, ferroelectric thin films, microwaves, spintronics, semiconductor technologies and memory devices* etc. These materials have been the subject of significant research interest because of the intriguing underlying physics showing marked colossal magnetoresistance (CMR) effect and the anticipated multifunctional and advanced applications for the next generation electronics. The recent discovery of large magnetoelectric effects in the $R_{1-x}A_xMnO_3$ (where R and A are trivalent rare earth and divalent alkaline earth ions, respectively) has kindled interest among investigators in understanding the complex relationships between lattice distortion, magnetism, dielectric and thermodynamic properties of undoped $RMnO_3$ and are good candidates for certain sensor applications, bolometers, magnetic refrigeration, read head devices, magnetic storage in hard disk and floppy disks, and spin valve devices (such as the 21st Century electronics i.e. spintronics (Yamasaki et al., 2007). The huge magnetoresistance or colossal magnetoresistance effect (CMR) has been observed in the perovskite manganites (Jin et al., 1994). The *magnetoresistance* is defined as $(\Delta R/R_H = [R(T,H) - R(T, 0)]/R(T, H)$. Magnetoresistance can be negative or positive. In most nonmagnetic solids the magnetoresistance is positive. In non-magnetic pure metals and alloys MR is generally positive and MR shows a quadratic dependence on H. MR can be negative in magnetic materials because of the suppression of "Spin Disorder" by the magnetic field. The Giant magnetoresistive effect GMR was recently discovered by Sir Peter Grünsberg (Germany) and Sir Albert Flert (France) (see photographs 1 and 2) and both of them were awarded Nobel Prize in the year 2007 (Baibich et al., 1988; Binasch et al., 1989). It has been used extensively in read heads of modern hard drives. Another application of the GMR effect is non-volatile, magnetic random access memory. Read heads of modern hard drives are based on the GMR or TMR effect.The GMR effect is observed, mainly, in artificial multilayer systems with alternating magnetic structure and is used in many applications. The large magnetoelectric effects in the rare-earth manganites $RMnO_3$ has reopened the field of the so-called *multiferroic materials.* Multiferroic means, that several ferro-type orders, such as ferromagnetism, ferroelectricity or ferroelasticity coexist.

1

2

Photograph 1. Peter Grünberg, 2. Albert Fert Nobel Prize Winners of 2007

Manganites have opened up challenging and exciting possibilities for research in condensed matter physics and materials science. Today, the science and technology of magnetism have undergone a renaissance, driven both by the urge to understand the new physics and by demand from industries for better materials. The current computer age relies on the development of smaller and "smaller" materials for memory devices, data storage, processing and probing. Materials can be divided into numerous categories, depending on their origin, use or morphology. The number of applications, properties and their combinations seems to be almost unlimited. One prime example of a small but diverse group of materials is the perovskite family. Solid state physicists, chemists and materials scientists have recently shown a wide interest in these perovskites, because of their unique properties such as the high temperature superconductivity, colossal magnetoresistance (CMR) and ferroelectricity. Still new and unexplored possibilities of the perovskites appear. In spite of the progress made in our understanding of the properties of these materials, very basic questions like "Why is this material a good conductor, while a similar material is an insulator" remain a challenge. Millions of people tackle this question everyday. Manganites clearly offer great opportunity at low temperatures but extending this promise to room temperature remains a challenge.

Despite enormous theoretical and experimental activity in the area of manganites, a complete understanding of the unusual physical properties in perovskite manganites is still lacking and many questions remain unresolved. For example, a lot of theoretical models are developed, but they are so diverse that it is difficult to choose between them. Moreover, a quantitative comparison of the known models with experimental data is practically impossible or too ambiguous. After several theoretical efforts in recent years, mainly guided by the computational and mean-field studies of realistic models, considerable progress has been achieved in understanding the physical properties of these compounds. Most vividly, to the best of my knowledge, only a few groups are involved with the theoretical investigation of the temperature, pressure and composition-dependent thermodynamical, structural and phonon dynamical (vibrational) properties of perovskite manganites and/or multiferroic manganites.

Recently, a modified rigid ion model (MRIM) has been developed by the author (Renu Choithrani et al., 2008-2010) to elucidate the cohesive, thermal and thermodynamic properties of pure and doped perovskite manganites and the study is recognized in journals of international repute with high impact factor, awarded and appreciated by the eminent scientists, Nobel Laureates, reputed national and international Universities, Research Centres and R & D groups.

The system offers a degree of chemical flexibility which permits the relation between the structural, electronic and magnetic properties of these oxides to be examined in a systematic way. The manganites also have potential as solid electrolytes, catalysts, sensors and novel electronic materials. Their rich electronic phase diagrams reflect the fine balance of interactions which determine the electronic ground state. These compounds represent the interplay of experiment, theory and application which is an important aspect of condensed matter physics research.

The experiments have given quantitative explanation of the metal-insulator phase transitions, while from a fundamental point of view, the central question is to understand the different physical properties and thus, the theoretical attempts are still awaited to understand the mechanism of these exotic materials. Looking to the importance of materials and availability of wealth of experimental data on various physical properties. It is well known that these physical properties of the materials originate from the interatomic interactions between their atoms. Therefore, the author has thought it pertinent to develop the model of interatomic potentials with limited number of adjustable parameters to predict the cohesive, thermal, elastic and phononic dynamical properties of the pure and doped perovskites. The perovskite structure is adopted by many oxides that have the chemical formula ABO_3. The relative ion size requirements for stability of the cubic structure are quite stringent, so slight buckling and distortion can produce several lower-symmetry distorted versions, in which the coordination numbers of A , B ions or both are reduced. The stability of the perovskite structure depends upon the tolerance factor defined by Goldsmith tolerance factor (t). The perovskite structure is supposed to be stabilized in the range of $0.75< t < 1$. However, for an ideal perovskite $t = 1$. For perovskite containing small central cations, the Goldschmidt tolerance factor, t, is typically <1. Tilting of the octahedral structure is common in perovskite with $t<1$. For $t<1$, the cubic structure transforms to the orthorhombic structure which leads to deviation in the Mn-O-Mn bond angle from 180^o (for an ideal perovskite). The deviation of the Mn-O-Mn bond angle from 180^o leads to the distortion in the MnO_6 octahedron. According to the Jahn-Teller (JT) theorem, the structure will distort thereby removing the degeneracy of the e_g orbitals. In solids, the orbital degree of freedom of the Mn^{3+} ion often shows long range ordering associated with the cooperative JT effect. The magnetic properties of the manganites are governed by exchange interactions between the Mn ion spins. These interactions are relatively large between two Mn spins separated by an oxygen atom and are controlled by the overlap between the Mn d-orbitals and O p-orbitals.

The present investigations provide several important information about their cohesive, thermal, elastic, phonon and vibrational properties and how these properties of pure and doped perovskite manganites vary at magnetic transitions. The learning of inter molecular interaction is important as it influences the stability and hardness of the material. It is also distinguished that the chemical stability is associated with cohesive energy. Compounds with higher cohesive energy generally have chemical stability. The study of atomic

vibrations in crystalline solids is a subject with a long and interesting history and over the years has been explored in all its aspects. The formal basis for the investigation of the vibrations, especially within the framework of the harmonic approximation, along with meritorious treatments in their own right has been presented in this chapter. The modified effective interaction potentials to explore various physical properties of these advanced, smart and novel materials are described in detail in this chapter.

2. Importance

The development of new and novel materials for technological applications has opened many doors to innovation in the 21st century. New magnetic and electronic materials in particular have helped to bring about the information revolution. Many physicists are interested in new materials because they can be used to study a new physical phenomenon. With respect to structure, these manganites have been grouped into the hexagonal phase (*P*63*cm*) with *R* (= Ho, Er, Tm, Yb, Lu or Y) (Yakel et al., 1963) having smaller ionic radius (r_R) and the orthorhombic structure (*Pnma*) with *R* (= La, Pr, Nd, Sm, Eu, Gd, Tb or Dy) (Gilleo et al., 1957) having larger (r_R)(figures 1 and 2).

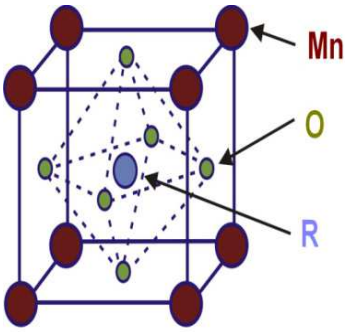

Fig. 1. Crystal lattice of the orthorhombic manganites $RMnO_3$.

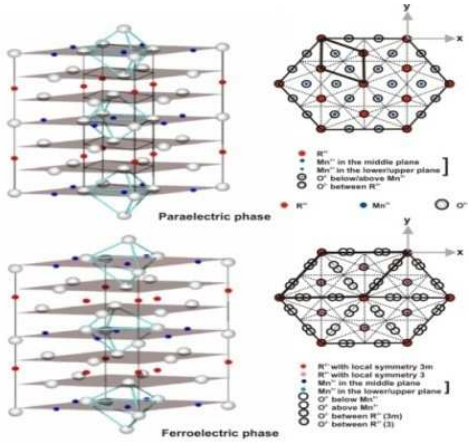

Fig. 2. Crystal lattice of the hexagonal manganites $RMnO_3$.

Research work on perovskite materials is being carried out both in India and other countries and has resulted into several important technological applications and patents, particularly in the areas like spintronics, semiconductor technologies, magnetic sensors, bolometers, magnetic refrigeration, read head devices, magnetic storage in hard disk and floppy disks. At the international level, an extensive research work is being conducted by several groups (Alonso et al., 2000; Lo´pez et al., 2002; Ku et al., 2004; Kimura et al., 2005; Iliev et al., 2006; Tachibana et al., 2007;) on pure and doped perovskite manganites. The research work in India is being conducted mostly at Indian Institute of Science, Bangalore (Prof. C.N.R. Rao and collaborators, 2001), Indian Institute of Technology, Delhi (Prof. H.C. Gupta and collaborators, 2008) Bhabha Atomic Research Centre, Mumbai (Prof. S.L. Chaplot and collaborators, 2011), and at several other organizations. Less theoretical attempts have been made to understand the mechanism. Interesting peculiar features are observed due to the effect of doping of rare earth (Ca, Sr, Ba,…..) in $RMnO_3$. Less attention has been paid on subterranean understanding of thermodynamic and phononic properties.

3. Detailed methodology

3.1 Extended Rigid Ion Model (ERIM)

The author has recently developed an extended rigid ion model (ERIM) by incorporating the the long-range (LR) Coulomb attraction, the short-range (SR) Hafemeister–Flygare (HF) type overlap repulsion effective up to the second neighbour ions, the van der Waals (vdW) attraction due to the dipole–dipole (d–d) and dipole–quadrupole (d–q) interactions and zero point energy (ZPE) effects in the framework of modified rigid ion model (MRIM) developed earlier by us(Renu Choithrani et al., 2008-2010).

The framework of ERIM is derived from the following interionic interaction potential:

$$\phi_{ERIM} = \phi_{MRIM} + \phi_{ZPE}$$

where, ϕ_{MRIM} potential (Renu Choithrani et al., 2008-2010) is given by

$$\phi_{MRIM} = -\frac{e^2}{2}\sum_{kk'} Z_k Z_{k'} r_{kk'}^{-1} + \left[\begin{array}{l} n b_1 \beta_{kk'} \exp\{(r_k + r_{k'} - r_{kk'})/\rho_1\} + \\ \frac{n'}{2} b_2 \left[\beta_{kk} \exp\{(2r_k - r_{kk})/\rho_2\} + \beta_{k'k'} \exp\{(2r_{k'} - r_{k'k'})/\rho_2\}\right] \end{array}\right] - \sum_{kk'} c_{kk'} r_{kk'}^{-6} - \sum_{kk'} d_{kk'} r_{kk'}^{-8} \quad (1)$$

and

$$\phi_{ZPE} = (9/4)\, K\theta_D \quad (2)$$

This ERIM has been developed and applied by the author, probably for the first time, to describe the thermodynamic and phononic properties of the doped and undoped perovskites materials.

$\beta_{kk'}$ are the Pauling coefficients:

$$\beta_{kk'} = 1 + (z_k / n_k) + (z_{k'} / n_{k'}) \tag{3}$$

with z_k ($z_{k'}$) and n_k ($n_{k'}$) as the valence and number of electrons in the outermost orbits of k (k′) ions. In Eqn. (1), $r_{kk'}$ and r_{kk}(= $r_{k'k'}$) are, respectively, the first and second neighbour separations and their values are obtained for A substitutions (x) using the well known Vegard's law (Vegard, 1921).

The symbols $c_{kk'}$ and $d_{kk'}$ are the corresponding vdW coefficients, whose values have been determined by using their expressions derived from the Slater-Kirkwood variational (SKV) (Slater & Kirkwood, 1931) method:

$$c_{kk'} = (3e\,\hbar\,\alpha_k\,\alpha_{k'} / 2m)\ [(\alpha_{k/Nk})^{1/2} + (\alpha_{k'/Nk'})^{1/2}]^{-1} \tag{4}$$

$$d_{kk'} = (27e\,\hbar^2\alpha_k\,\alpha_{k'} / 8m)\,[(\alpha_{k/Nk})^{1/2} + (\alpha_{k'/Nk'})^{1/2}]^2 \tag{5}$$

$$[(\alpha_{k/Nk})^{1/2} + 20/3\ (\alpha_k\,\alpha_{k'/\,Nk\,Nk'})\ (\alpha_{k'/Nk'})]^{-1}$$

where m and e are the mass and charge of electron, respectively. a_k($a_{k'}$) are the electronic polarizabilities of k(k′) ions ; N_k ($N_{k'}$) are the effective number of electrons responsible for the polarization of k(k′) ions. The values of $c_{kk'}$ and $d_{kk'}$ are evaluated using the Eqns. (4) and (5) and the procedure prescribed in our earlier papers (Renu Choithrani et al., 2008-2010).

The model parameters (hardness (b) and range (ρ)) are determined from the equilibrium condition:

$$[\,d\phi(r) / dr\,]_{r=r_0} = 0 \tag{6}$$

and the Bulk modulus:

$$B = (9Kr_0)^{-1}[d^2\phi(r) / dr^2]_{r=r_0} \tag{7}$$

here, r_o and r are the interionic separations in the equilibrium and otherwise states of the system, respectively. The symbol K is the crystal structure constant.

The total specific heat is computed by including the contribution of specific heat from lattice, electrons, phonons and schottky effects.

$$C_{lat} = 9RN(\frac{T}{\theta_D})\int_0^{\theta_D/T} \frac{x^4 e^x}{(e^x - 1)^2} dx \tag{8}$$

where N=5 is the number of atoms in the unit cell, R = 8.314 J /mol K is the ideal gas constant, θ_D is the Debye temperature and x = θ_D /T.

$$C_p = C_e + C_{ph} + C_{sch} \tag{9}$$

$$C_e = \gamma T \tag{10}$$

$$C_{ph} = \beta T^3 \tag{11}$$

$$C_{sch} = \frac{R}{T^2}\left\{\sum_{i=1}^{n}\Delta_i^2 \exp(\frac{-\Delta_i}{T}) / \sum_{i=1}^{n}\exp(\frac{-\Delta_i}{T}) - \left[\sum_{i=1}^{n}\Delta_i \exp(\frac{-\Delta_i}{T}) / \sum_{i=1}^{n}\exp(\frac{-\Delta_i}{T})\right]^2\right\} \tag{12}$$

The computations have been performed to understand the cohesive and thermal properties at different temperatures (T) and compositions (x) of $RMn_{1-x}Ga_xO_3$ (R = Ho, Y and x =0, 0.03, 0.1, 0.2 and 0.3). Here, the author has tried to address the study of thermodynamic properties of solids which is one of the fascinating fields of condensed matter physics in the recent years. Thermodynamics play an important role in explaining the behaviour of manganites, as many properties are attributed to 'electron–phonon' interaction. As electron–phonon interaction is one of the most relevant contributions in determining the conduction mechanism in these materials. The strong coupling between the electron and the lattice brings about by a small change in the chemical composition, like the ratio between trivalent and divalent ions at the A site or the average ionic radius of the ions on the A site, a large changes in the physical properties. Thus, the thermodynamic and phononic properties of these materials may be taken as a starting point to a consistent understanding of the more complex physical properties of the manganites. The author has explored the physical properties such as cohesive energy (ϕ), molecular force constant (f), compressibility (β), Restrahalen frequency (υ_0), Debye temperature (θ_D), Grüneisen parameter (γ) and specific heat (C(T)), probably for the first time, using extended rigid ion model (ERIM).

4. Results and discussion

Using the input data (Zhou et al., 2006) and the vdW coefficients ($c_{kk'}$ and $d_{kk'}$) calculated from the SKV method, the model parameters ((b_1, ρ_1) and (b_2, ρ_2)) corresponding to the ionic bonds Mn-O and R/Ga–O for different compositions ($0.0 \le x \le 0.3$) and temperatures 0 K $\le$ T $\le$ 300 K have been calculated using equations (6) and (7) for $RMn_{1-x}Ga_xO_3$ (R = Ho, Y and x = 0, 0.03, 0.1, 0.2 and 0.3). Using the disposable model parameters listed in tables 1 and 2, the values of ϕ, f , β, υ_0, θ_D and γ are computed and depicted in tables 3 and 4 for $RMn_{1-x}Ga_xO_3$ (R = Ho, Y and x = 0, 0.03, 0.1, 0.2 and 0.3), respectively. The chief aim of the application of the present model is to reproduce the observed physical properties such as the phononic and thermodynamic properties of perovskite manganites. Keeping this objective in view, we find that our results obtained for most of these properties are closer to the experimental data (Zhou et al., 2006) available only at 300 K. The cohesive energy is the measure of strength of the force binding the atoms together in solids. This fact is exhibited from cohesive energy results which follow the similar trend of variation with *T*, as is revealed by the bulk modulus that represents the resistance to volume change. This feature is indicated from tables 3 and 4, which show that the values of the cohesive energy (ϕ) decreases from −148.01 eV for $HoMn_{1-x}Ga_xO_3$ (x = 0) to −149.52 eV for $HoMn_{1-x}Ga_xO_3$ (x = 0.2) and −146.99 eV for $YMn_{1-x}Ga_xO_3$ (x = 0) to −148.87 eV for $YMn_{1-x}Ga_xO_3$ (x = 0.3) dopings; the same trend of variation is also exhibited by the bulk modulus. Due to a lack of experimental data, the values of cohesive energy of $RMn_{1-x}Ga_xO_3$ (R = Ho, Y and x =0, 0.03, 0.1, 0.2 and 0.3) are compared with that of $LaMnO_3$ (De Souza et al., 1999), which is a member of the same family. The negative values of cohesive energy show that the stability

of these manganites is intact. It is also noticed from tables 1 and 2 that the values of hardness (b_1, b_2) and range parameters (ρ_1, ρ_2) increase with concentrations (x). The author has also calculated the values of the molecular force constants (f) and Restrahalen frequencies (υ_0) (see tables 3 and 4) and found that υ_0 increases with temperatures (T) and concentrations (x). Since the Restrahalen frequency is directly proportional to the molecular force constant (f) therefore both of them vary with the temperature accordingly for different concentrations (x). The values of Restrahalen frequency are almost in the same range as that reported for the pure material $YMnO_3$ (υ_0 = 13.08 THz) (Zhou et al., 2006). The calculated value of Debye temperature (θ_D) for $RMn_{1-x}Ga_xO_3$ (R = Ho, Y and x =0, 0.03, 0.1, 0.2 and 0.3) is approximately in agreement and comparable with the corresponding data (577 K and 628 K) available only at room temperature for $HoMnO_3$ and $YMnO_3$ (Zhou et al., 2006; Renu Choithrani et al., 2011). The calculated values of (θ_D) for $RMn_{1-x}Ga_xO_3$ (R = Ho, Y and x =0, 0.03, 0.1, 0.2 and 0.3) at 300 K are ranging from 577.11 K to 622.05 K, which lie within the Debye temperature range (300–650 K) often found in perovskite manganites (Renu Choithrani et al., 2008-2010). The Grüneisen parameters (γ) obtained by the author are found to lie between 2 and 3, which are similar to the values observed by Dai et al., 1996.

The specific heat (C) values calculated by the author for $RMn_{1-x}Ga_xO_3$ (R = Ho, Y and x =0, 0.03, 0.1, 0.2 and 0.3) at temperatures 0 K ≤ T ≤ 300 K and are displayed in figures 3-11 and found to be in good agreement with the measured data (Zhou et al., 2006). The computed results have followed a trend more or less similar to those exhibited by the experimental curve at lower temperatures. A sharp peak is observed in the experimental specific heat curve at ~59 K due to the A-type AF ordering. The change in Mn–O distance by the substitution of a Ga increases θ_D and hence there is a consistent decrease in the specific heat values corresponding to the doping in both of the cases (see figures 3-11). Hence, the concentration (x) dependence of θ_D in $RMn_{1-x}Ga_xO_3$ (R = Ho, Y and x =0, 0.03, 0.1, 0.2 and 0.3) suggests that increased doping drives the system effectively towards the strong electron–phonon coupling regime. The present ERIM calculations yield similar specific heat values at low temperatures (below 60 K) where the acoustic phonons play an important role. On doping Ga (x = 0, 0.03, 0.1 and 0.2) in $HoMnO_3$, the specific heat increases monotonically with temperature as shown in figures 3-11. The experimental specific heat results (Zhou et al., 2006) and the computed values by ERIM for $HoMn_{1-x}Ga_xO_3$ (x =0, 0.03, 0.1 and 0.2) show three anomalies: (i) a λ-type anomaly at T_N , below 65 K(ii) a narrow peak around T_{SR}, , below 40 K and (iii) a sharp peak at T_2, below 5 K. With increasing the concentration (x), T_N and T_2 decrease but T_{SR} increases. It is also seen from figures 3-6 that the theoretical results obtained by ERIM are in closer agreement with the available experimental (Zhou et al., 2006) data. It is noticed from figures 7-11, the specific heat of $YMn_{1-x}Ga_xO_3$ just shows a λ-type peak at T_N, which decreases with increasing x. For the $YMn_{1-x}Ga_xO_3$ (x =0, 0.03, 0.1, 0.2 and 0.3) materials, the specific heat curve shows no peak with temperature down to 2 K. Another noteworthy feature is that there are broad peaks between 5 K and 10 K for $HoMn_{1-x}Ga_xO_3$, but no such peaks for $YMn_{1-x}Ga_xO_3$. The ERIM results have fairly well reproduced the experimental specific heat data in the temperature ranges 100 K ≤ T ≤ 250 K except for the range 250 K ≤ T ≤ 300 K, in which the experimental specific heat values are not available (see figures 3-11); this feature corresponds to the phase transition from a second-order nature of the antiferromagnetic (AFM) transition of the Mn^{3+} magnetic moments as revealed from the

specific heat measurements were performed on a PPMS (Physical Property Measurement System, Quantum Design) data (Zhou et al., 2006).

5. Tables and figures

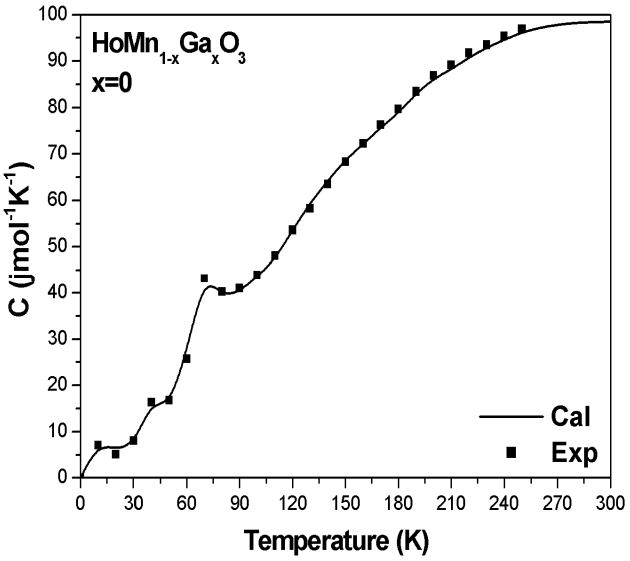

Fig. 3. The specific heat of $HoMn_{1-x}Ga_xO_3$ (x = 0) as a function of temperature.

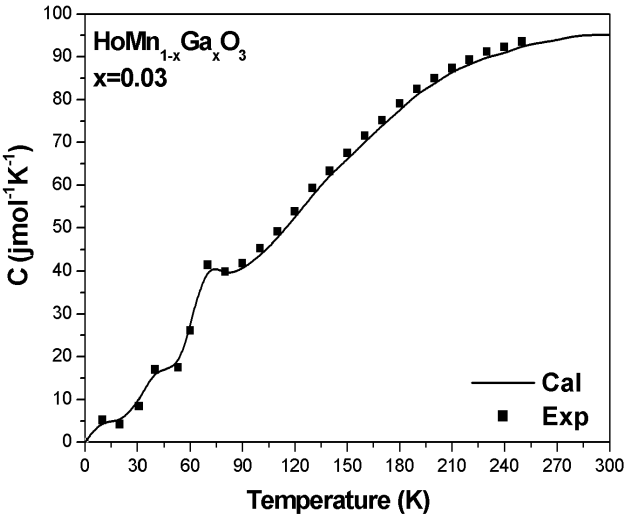

Fig. 4. The specific heat of $HoMn_{1-x}Ga_xO_3$ (x = 0.03) as a function of temperature.

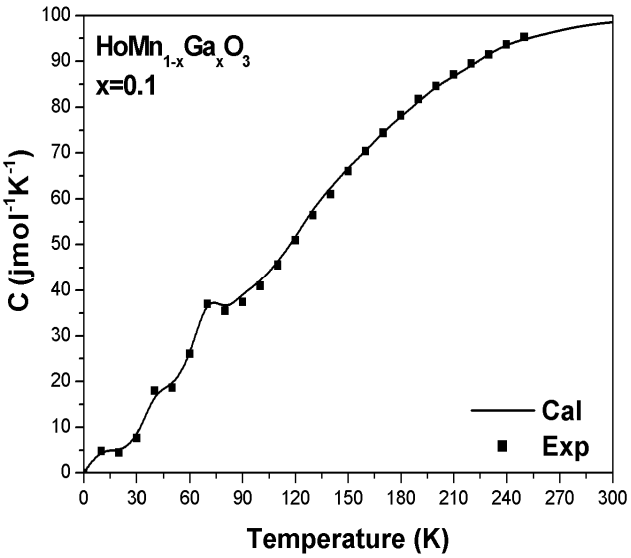

Fig. 5. The specific heat of $HoMn_{1-x}Ga_xO_3$ (x = 0.1) as a function of temperature.

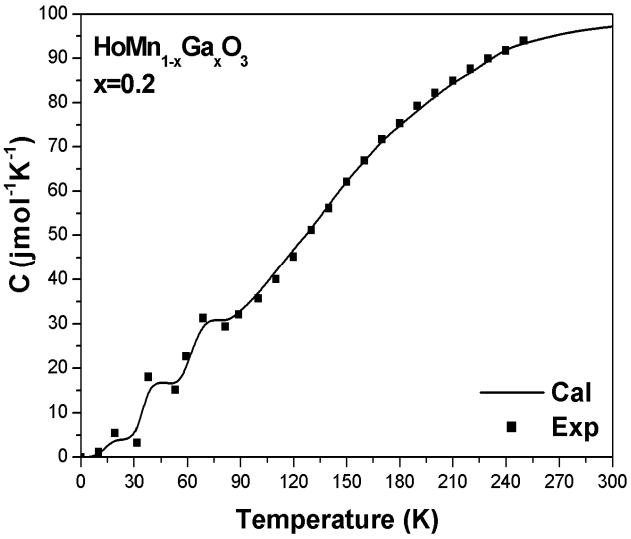

Fig. 6. The specific heat of $HoMn_{1-x}Ga_xO_3$ (x = 0.2) as a function of temperature.

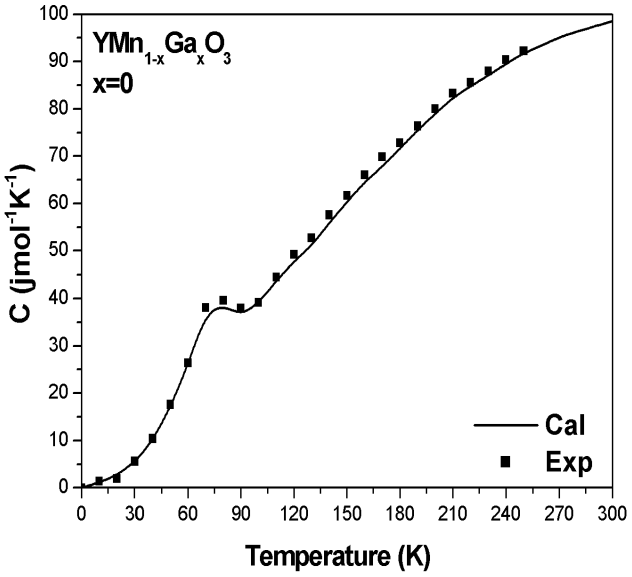

Fig. 7. The specific heat of $YMn_{1-x}Ga_xO_3$ (x = 0) as a function of temperature.

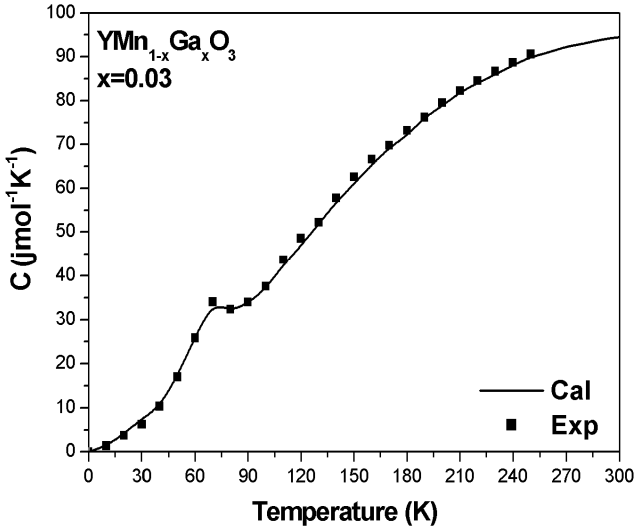

Fig. 8. The specific heat of $YMn_{1-x}Ga_xO_3$ (x = 0.03) as a function of temperature.

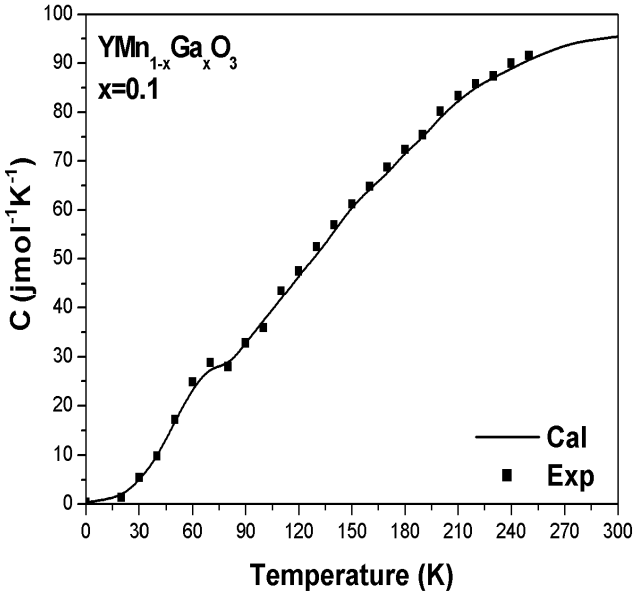

Fig. 9. The specific heat of $YMn_{1-x}Ga_xO_3$ (x = 0.1) as a function of temperature.

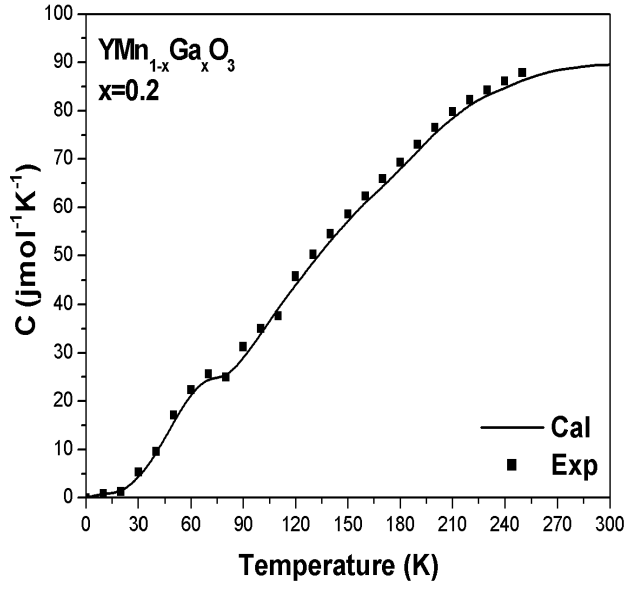

Fig. 10. The specific heat of $YMn_{1-x}Ga_xO_3$ (x = 0.2) as a function of temperature.

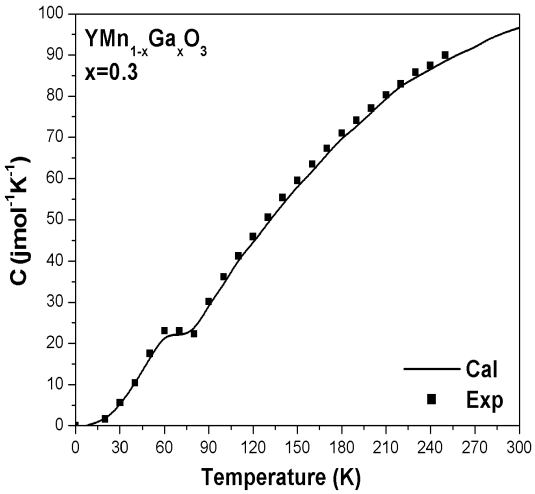

Fig. 11. The specific heat of $YMn_{1-x}Ga_xO_3$ (x = 0.3) as a function of temperature.

Concentration (x)	Model parameters			
	Mn-O		Ho/Ga-O	
	b_1 (10^{-12} erg)	ρ_1 (Å)	b_2 (10^{-12} erg)	ρ_2 (Å)
0	1.907	0.602	2.023	0.702
0.03	1.932	0.609	2.110	0.717
0.1	1.950	0.610	2.120	0.719
0.2	1.976	0.612	2.146	0.720

Table 1. The model parameters of $HoMn_{1-x}Ga_xO_3$ ($0 \le x \le 0.2$)

	Model parameters			
Concentration (x)	Mn-O		Y/Ga-O	
	b_1 (10^{-12} erg)	ρ_1 (Å)	b_2 (10^{-12} erg)	ρ_2 (Å)
0	1.981	0.8902	3.183	0.991
0.03	1.986	0.8922	3.197	0.994
0.1	1.991	0.8945	3.224	0.996
0.2	1.996	0.9445	3.294	0.997
0.3	2.001	0.9479	3.299	0.999

Table 2. The model parameters of $YMn_{1-x}Ga_xO_3$ ($0 \le x \le 0.3$)

(x)	ϕ (eV)	f (10^4 dyne.cm^{-1})	β (10^{-12} dyn^{-1}.cm^2)	υ_0 (THz)	θ_D (K)	γ
0	-148.01	20.09	1.87	12.02	577.11	2.10
0.03	-148.42	20.76	1.89	12.06	578.99	2.12
0.1	-149.39	21.51	1.91	12.07	579.67	2.17
0.2 (Expt.)	-149.52 (-141.81)	21.97	1.99	12.10	581.12 (577)	2.19 (2-3)

Table 3. Thermophysical properties of $HoMn_{1-x}Ga_xO_3$ ($0 \le x \le 0.2$)

(x)	ϕ (eV)	f (10^4 dyne.cm^{-1})	β (10^{-12} dyn^{-1}.cm^2)	υ_0 (THz)	θ_D (K)	γ
0	-146.99	24.56	2.01	12.89	618.68	2.971
0.03	-147.01	24.89	2.04	12.91	619.77	2.977
0.1	-147.59	24.97	2.17	12.92	620.24	2.982
0.2	-148.19	25.29	2.19	12.94	621.16	2.989
0.3 (Expt.)	-148.87 (-141.81)	25.99	2.21	12.95 (13.08)	622.05 (628)	2.990 (2-3)

Table 4. Thermophysical properties of $YMn_{1-x}Ga_xO_3$ ($0 \le x \le 0.3$)

6. Conclusion

On the basis of the overall descriptions, it may be concluded that the diverse exposition of the temperature-dependent thermodynamical and phononic properties of perovskite manganites $RMn_{1-x}Ga_xO_3$ (R = Ho, Y and x =0, 0.03, 0.1, 0.2 and 0.3) attained by the author is remarkable in view of the inherent simplicity of the extended rigid ion model. All this indicates the power and usefulness of the ERIM as having the potential to explain a variety of physical properties (such as cohesive, thermal, elastic and thermodynamic) of the pure and doped perovskite materials. However, the efforts that have been devoted by many experimental workers to observe magnetic transitions and properties, to the best of my knowledge, only a few groups are involved with the study of temperature- and composition-dependent properties of perovskite manganites (or CMR) materials. The extended rigid ion model has reproduced the physical properties that correspond well to the experimental data. The author believes that such properties will serve young researchers, scientists and experimental workers fruitfully. Also, they will get additional informations i.e. more than a thermodynamical and vibrational picture of these materials. However, it is expected to be of immense use to other workers with peripheral interest in thermodynamical and phononic. ERIM has been applied to compute the cohesive, thermal and thermodynamical properties of the pure and doped perovskites. Some of the results on these physical properties of $RMn_{1-x}Ga_xO_3$ (R = Ho, Y and x =0, 0.03, 0.1, 0.2 and 0.3) are, probably, reported for the first time. These theoretical results are of academic interest as well as of help to understand the mechanism of CMR materials. The success of the model in predicting thermodynamic and phononic properties depends crucially on their ability to explain a variety of microscopic and macroscopic dynamical properties of such complex structured materials.

7. Acknowledgments

I would like to acknowledge with thanks the Science and Engineering Research Board, Department of Science and Technology (DST), Government of India, New Delhi for providing the financial assistance and the Fast Track Young Scientist Award. It would be noteworthy to thank Dr. N.K. Gaur for his constant encouragement during the tenure of my study.

8. References

Alonso, J.A., Martı´nez-Lope, M.J., Casais, M.T., & Ferna´ndez-Dı´az, M.T. (2000). Evolution of the Jahn-Teller distortion of MnO6 octahedra in $RMnO_3$ perovskites (R) Pr, Nd, Dy, Tb, Ho, Er, Y): A neutron diffraction study, *Inorg. Chem.* Vol.(39): 917.

Baibich, M.N., Broto, J.M., Fert, A., Nguyen, F., Dau, Van, Petroff, F., Eitenne, P., Creuzet, G., Friederich, A., & Chazelas (1988). Giant magnetoresistance of (001)Fe/(001)Cr magnetic superlattices, J. *Phys. Rev. Lett.* Vol.(61): 2472.

Binasch, G., Grünberg, P., Saurenbach F., & Zinn, W. (1989). Enhanced magnetoresistance in layered magnetic structures with antiferromagnetic interlayer exchange, *Phys. Rev. B* Vol.(39): 4828.

Choithrani, Renu, & Gaur, N.K. (2008). Analysis of low temperature specific heat in $Nd_{0.5}Sr_{0.5}MnO_3$ and $R_{0.5}Ca_{0.5}MnO_3$ (R=Nd, Sm, Dy and Ho) compounds, *J. Magn. Magn. Mater.* Vol.(320): 3384.

Choithrani, Renu, & Gaur, N.K. (2008). Heat capacity of $EuMnO_3$ and $Eu_{0.7}A_{0.3}MnO_3$ (A =Ca, Sr) compounds, *J. Magn. Magn. Mater.* Vol.(320): 10.

Choithrani, Renu, Gaur, N.K., & Singh, R.K. (2008). Specific heat and transport properties of $La_{1-x}Gd_xMnO_3$ at 15 K ≤ T ≤ 300 K, *Solid. State Commun.* Vol.(147): 103.

Choithrani, Renu, Gaur, N.K., & Singh, R.K. (2008). Thermodynamic properties of $SmMnO_3$, $Sm_{0.55}Sr_{0.45}MnO_3$ and $Ca_{0.85}Sm_{0.15}MnO_3$, *J. Phys.: Condens. Matter* Vol.(20): 415201.

Choithrani, Renu, & Gaur, N.K. (2008). Thermo physical properties of multiferroic rare earth manganite $GdMnO_3$, *AIP Proc.* Vol.(1004): 73.

Choithrani, Renu, Gaur, N.K., & Singh, R.K. (2009). Study of calcium doping effect on thermophysical properties of some perovskite manganites, *J. Alloys and Compounds* Vol.(480): 727.

Choithrani, Renu, Gaur, N.K., & Singh, R.K. (2009) . Influence of temperature and composition on cohesive and thermal properties of mixed crystal manganites, *J. Magn. Magn. Mater.* Vol.(321): (2009) 4086.

Choithrani, Renu, & Gaur, N.K. (2010). Specific heat of Cd-doped manganites, *J. Comput. Mat. Sci.* Vol.(49): 107.

Choithrani, Renu, Rao, Mala N, Chaplot, S.L., Gaur, N. K., & Singh, R. K. (2011). Lattice dynamics of manganites $RMnO_3$ (*R* = Sm, Eu or Gd): instabilities and coexistence of orthorhombic and hexagonal phases, New *J. Phys* Vol.(11): 073041; (2009). Structural and phonon dynamical properties of perovskite manganites: (Tb,Dy, Ho)MnO_3, *Journal of Magnetism and Magnetic Materials* Vol.(323): 1627.

Dai, P., Jiandi, Zhang, Mook, H.A., Lion, S.H., Dowben, P.A., & Plummer, E.W. (1996). Experimental evidence for the dynamic Jahn-Teller effect in $La_{0.65}Ca_{0.35}MnO_3$, *Phys.Rev. B* Vol.(54): 3694(R).

De Souza, Roger A., Islam, S., M., & Tiffe, E.I. (1999). Formation and migration of cation defects in the perovskite oxide $LaMnO_3$, *J. Mater. Chem.* Vol.(9) : 1621.

Gilleo, M.A. (1957). Crystallographic studies of perovskite-like compounds. III. La(M_x, Mn_{1-x})O_3 with M = Co, Fe and Cr, *Acta Crystallogr.* Vol.(10): 161.

Gupta, H.C., & Tripathi, U. (2008). Zone center phonons of the orthorhombic $RMnO_3$ (R = Pr, Eu, Tb, Dy, Ho) perovskites, *PMC Physics B* Vol.(1): 9.

Iliev, M.N., Abrashev, M.V., Laverdière, J., Jandl, S., Gospodinov, M.M., Wang, Y.-Q., & Sun, Y.-Y. (2006). Distortion-dependent Raman spectra and mode mixing in $RMnO_3$ perovskites (R=La,Pr,Nd,Sm,Eu,Gd,Tb,Dy,Ho,Y), *Phys.Rev. B* Vol.(73): 064302.

Jin, S., Tiefel, T.H., McCormack, M., Fastnacht, R.A., Ramesh, R. & Chen, L.H. (1994). Thousandfold change in resistivity in magnetoresistive La-Ca-Mn-O films, *Science* Vol.(264): 413.

Kimura, T., Lawes, G., Goto, T., Tokura, Y., & Ramirez, A.P. (2005). Magnetoelectric phase diagrams of orthorhombic $RMnO_3$ (R = Gd, Tb, and Dy), *Phys. Rev. B* Vol.(71): 224425.

Ku, H.C., Chen, C.T., & Lin, B.N. (2004). A-type antiferromagnetic order, 2D ferromagnetic fluctuation and orbital order in stoichiometric $La_{1-x}Eu_xMnO_3$, *J. Magn. Magn. Mater.* Vol.(272): 85.

Lo´pez, J., de Lima, O.F., Lisboa-Filho, P.N., & Araujo-Moreira, F.M. (2002). Specific heat at low temperatures and magnetic measurements in $Nd_{0.5}Sr_{0.5}MnO_3$ and $R_{0.5}Ca_{0.5}MnO_3$ (R=Nd, Sm, Dy, and Ho) samples, *Phys. Rev. B* Vol.(66): 214402.

Raychaudhuri, A.K., Guha, A., Das, I., Rawat, R., & Rao, C.N.R. (2001). Specific heat of single-crystalline $Pr_{0.63}Ca_{0.37}MnO_3$ in the presence of a magnetic field, *Phys. Rev. B* Vol.(64): 165111.

Slater, J.C., & Kirkwood, K.G. (1931). The van der Waals forces in gases, *Phys. Rev. Lett.* Vol.(37): 682.

Tachibana, M., Shimoyama, T., Kawaji, H., Atake, T., & Muromachi, E. T. (2007). Jahn-Teller distortion and magnetic transitions in perovskite $RMnO_3$ (R=Ho, Er, Tm, Yb, and Lu), *Phys.Rev. B* Vol.(75): 144425.

Vegard, L. (1921). The constitution of mixed crystals and filling the space of atoms, *Z. Phys.* Vol.(5): 17.

Yakel, H.L., Koehler, W.C., Bertaut, E.F., & Forrat, E.F. (1963). On the crystal structure of the manganese(III) trioxides of the heavy lanthanides and yttrium, *Acta Crystallogr.* Vol.(16): 957.

Yamasaki, Y., Miyasaka, S., Goto, T., Sagayama, H., Arima, T. & Tokura, Y. (2007). Ferroelectric phase transitions of 3d-spin origin in $Eu_{1-x}Y_xMnO_3$, *Phys. Rev. B* Vol.(76): 184418.

Zhou, H.D., Janik, J. A., Vogt, B. W., Jo, Y. J., Balicas, L., Case, M. J., Wiebe, C. R., Denyszyn, J. C., Goodenough, J. B., & Cheng, J. G. (2006). Specific heat of geometrically frustrated and multiferroic $RMn_{1-x}Ga_xO_3$ (R=Ho,Y), *Phys.Rev. B* Vol. (74): 094426.

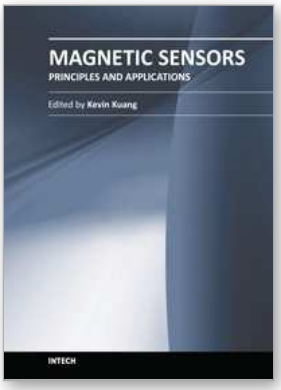

Magnetic Sensors - Principles and Applications

Edited by Dr Kevin Kuang

ISBN 978-953-51-0232-8
Hard cover, 160 pages
Publisher InTech
Published online 09, March, 2012
Published in print edition March, 2012

This book provides an introductory overview of the research done in recent years in the area of magnetic sensors. The topics presented in this book range from fundamental theories and properties of magnets and their sensing applications in areas such as biomedicine, microelectromechanical systems, nano-satellites and pedestrian tracking. Written for the readers who wished to obtain a basic understanding of the research area as well as to explore other potential areas of applications for magnetic sensors, this book presents exciting developments in the field in a highly readable manner.

InTech Europe
University Campus STeP Ri
Slavka Krautzeka 83/A
51000 Rijeka, Croatia
Phone: +385 (51) 770 447
Fax: +385 (51) 686 166
www.intechopen.com

InTech China
Unit 405, Office Block, Hotel Equatorial Shanghai
No.65, Yan An Road (West), Shanghai, 200040, China
中国上海市延安西路65号上海国际贵都大饭店办公楼405单元
Phone: +86-21-62489820
Fax: +86-21-62489821